Beam control in tri-core photonic lattices*

Ye Zhuo-Yi(叶卓艺)[a)b)], Xia Shi-Qiang(夏世强)[a)], Song Dao-Hong(宋道红)[a)], Tang Li-Qin(唐莉勤)[a)†], and Lou Ci-Bo(楼慈波)[a)]

[a)] *The MOE Key Laboratory of Weak Light Nonlinear Photonics, TEDA Applied Physics School and School of Physics, Nankai University, Tianjin* 300457, *China*

[b)] *Innovation Center, Bureau of Economic Development and Administrative Approval, Ningbo–Hangzhou Bay New Zone Administrator Committee, Ningbo* 315336, *China*

(Received 11 March 2013; revised manuscript received 30 May 2013; published online 20 December 2013)

We report on theoretical investigations of beam control in one-dimensional tri-core photonic lattices (PLs). Linear splitting is illustrated in tri-core PLs; the effect of defect strength on the splitting is discussed in depth for single-wavelength light. We reveal that splitting disappears when the defect strength trends to zero, while reoccurring under nonlinearity. Multi-color splitting and active control are also proposed in such photonic structures.

Keywords: tri-core photonic lattices, splitting

PACS: 42.65.–k, 42.65.Wi, 42.65.Tg **DOI:** 10.1088/1674-1056/23/2/024211

1. Introduction

In the past decade, photonic band-gap structures (PBGs), including photonic crystals (PCs) and periodic waveguide arrays, have attracted great attention due to their fundamental physics and potential applications.[1–3] All this research, based on total internal reflection, mainly focused on high refractive indices with little work on low refractive indices. However, the behavior of light in the low index regime, such as band-gap guiding due to Bragg reflection, is also fascinating and has many advantages.[4–7] Light bending in the sharp low refractive index corners exhibits lossless transmission while light bending for high indices or conventional waveguides always suffer from energy losses by leaking.[8] Single defect modes, both in theory and experiment,[9,10] have been widely discussed. Some potential applications, such as the circling, redirecting and blocking of light beams, are also demonstrated in defected PLs and PCs.[11–13] Furthermore, dual-core photonic crystal fiber (PCF) couplers in optical communication[14–17] and optical switching between two low-index sites[18] have been investigated. Broad-band trapping and splitting of light beams and surface plasmon polaritons (SPPs) due to the adiabatic photonic bandgap in the time domain are also realized.[19–21] The problem of dual-core couplers is easiest for two-level systems. The extension to the three-level system of optical waveguide arrays with low refractive index sites is a more complicated task. We will demonstrate a way to split the monochromatic and multi-color light by introducing tri-core photonic lattices.

2. Theoretical model

In this paper, we numerically study the control and dynamic characteristics of light beams in one-dimensional tri-core PLs by exploiting the optical analogy between three-level systems and tri-core PLs. The structural parameter domain and the coupling length for beam splitting and combining in the tri-core PLs are discussed in depth. Moreover, with the same parameters, nonlinear splitting is demonstrated while it disappears in the linear region. In addition, multi-color splitting is revealed for the structure under discussion.

We begin from the governing equation for the complex amplitude of the field q of a monochromatic light beam propagating in a medium with a shallow transverse refractive index modulation that can be derived from Maxwell equations for a dielectric medium with Kerr nonlinearity. In the spirit of the slowly varying amplitude approximation, we have to deal with the following nonlinear Schrödinger equation:

$$\mathrm{i}\frac{\partial q}{\partial \xi} = -\frac{1}{2}\frac{\partial^2 q}{\partial \eta^2} + \sigma|q|^2 - pR(\eta)q. \tag{1}$$

Here the transverse η and longitudinal ξ coordinates are scaled to the characteristic beam width and diffraction length, respectively; the parameter p characterizes the lattice modulation strength; and the function $R(\eta)$ describes the refractive index profile. In our case,

$$\begin{aligned} R(\eta) = {} & \{1+h_{\mathrm{D}}f_{\mathrm{D}}(\eta)\}\{1+h_{\mathrm{D}}f_{\mathrm{D}}(\eta-L_s)\} \\ & \times\{1+h_{\mathrm{D}}f_{\mathrm{D}}(\eta+L_s)\}\{1+\cos(2\pi\eta/T)\} \end{aligned} \tag{2}$$

*Project supported by the State Key Program for Basic Research of China (Grant Nos. 2013CB632703 and 2010CB934101), the National Natural Science Foundation of China (Grant Nos. 10904078 and 60908002), the International Science & Technology Cooperation Program of China (Grant No. 2011DFA52870), the International Cooperation Program of Tianjin (Grant No. 11ZGHHZ01000), the "111" Project (Grant No. B07013), the Program for New Century Excellent Talents in University of China (Grant No. NCET-10-0507), and the Specialized Research Fund for the Doctorial Program of Higher Education of China (Grant No. 20120031120031).

†Corresponding author. E-mail: tanya@nankai.edu.cn

© 2014 Chinese Physical Society and IOP Publishing Ltd

describes the tri-core PLs with three low-index defect sites imprinted in a uniform lattice [Fig. 1(a1)], f_D is a localized function describing the shape of the defect and h_D controls the strength of the defect.[5] The length $L_s = nT$ is the spacing of the defected sites, consisting of n lattice periods T. The parameter $\sigma = \pm 1$ defines the type of nonlinearity (defocusing or focusing).

Three negative site defects are introduced by removing the refractive index modulation; we obtain the eigenmodes localized at the line defects [Figs. 1(a1) and 1(a2)] with the propagation constants located in the photonic bandgap. Note that there are three defect modes and we only show two of them here because they are associated with beam splitting dynamics. In a future publication, we plan to discuss the last one and some of its relevant propagation properties. In Figs. 1(a1) and 1(a2), the $a2$ mode has a staggered phase at the low-index site while the $a1$ mode is in phase. To explore in depth, we show that the propagation constants of the two modes depend on different separations of the defect sites. We find that the propagation constants of the two modes flip up and down alternately [see Fig. 1(b)]. Both are leading to an exponential decrease to a constant value when the separation is too far, arising from the degeneration of the system. We also study the system under different physical parameters, such as lattice strength (p) and defect strength (h_D). We obtain the zone [Fig. 1(c)] where the two modes coexist. Note that this zone is very important to help us clarify the beam propagation features in this system.

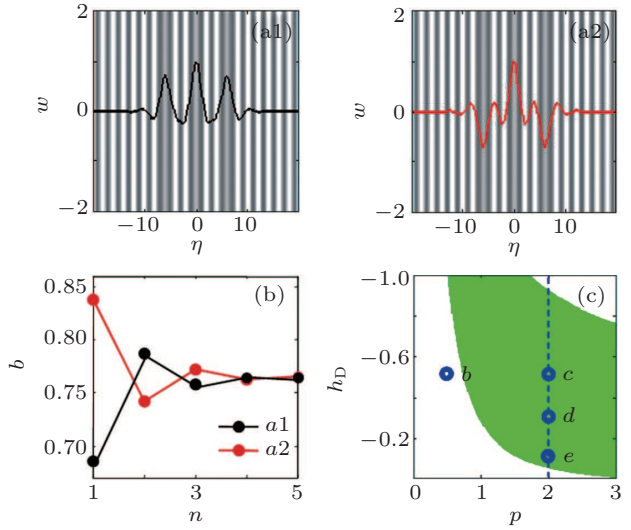


Fig. 1. (color online) (a1) and (a2) Profiles of $a1 = 0.741$ (black line) and $a2 = 0.788$ (red line) linear modes supported by the tri-core PLs at $p = 2$ and $L_s = 3T$. (b) Propagation constants versus number of lattice periods between cores at $p = 2$. (c) Green regions show the structure parameters at which splitting occur in gap 1. Blue circles (b–e) represent the structural parameters of the splitting dynamics in Fig. 2, respectively. All quantities are plotted in arbitrary dimensionless units.

3. Linear and nonlinear splitting dynamics

In the beam propagation simulation, we launch a Gaussian beam into the central defect site of the tri-core PLs with defect separation $3T$. When the parameters (lattice strength p and defect strength h_D) are located outside the zone indicated by circle b in Fig. 1(c), the output beam experiences strong diffraction [see Fig. 2(b)]. When the parameters are inside the zone, typical examples of splitting and combining dynamics in the tri-core PLs are depicted in Figs. 2(c) and 2(d) for different system parameters indicated by the circle c–d in Fig. 1(c). Light exited in the central defect site is slowly tunneling into two low-index neighborhood channels. After a certain propagation length, light energy is totally transferred to both defect sites close to the central one, and then backward tunneling sets on to where it was launched initially. The light splitting and combining dynamics is arising from $a1$ and $a2$ modes constructive or destructive interference during propagation. Thus the coexistence of these two defect modes plays an important role in the coupling and splitting dynamics. The coupling length L_c is an important parameter that describes the splitting dynamic characteristics. It is based on the difference between the corresponding propagation constants. With fixed $p = 2$,

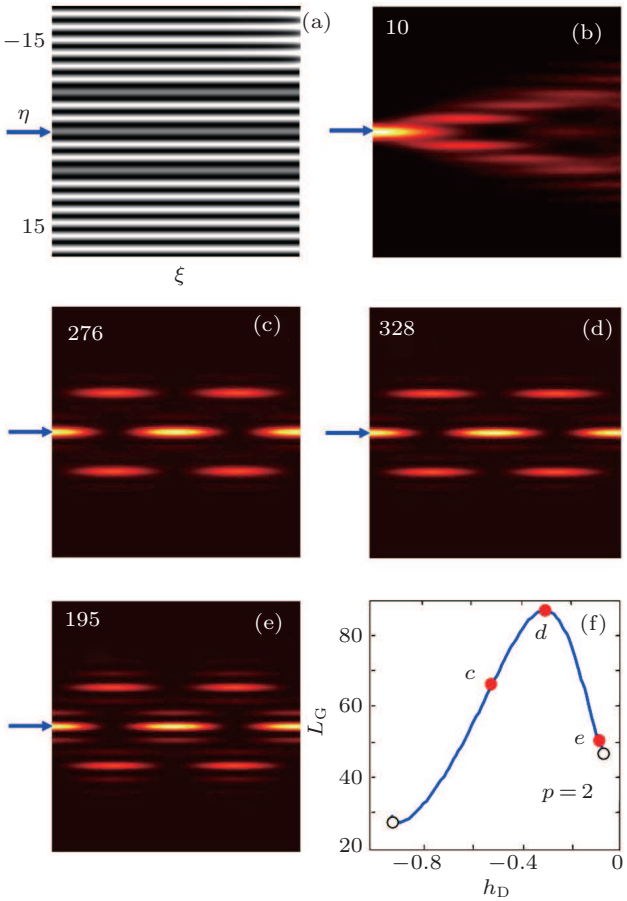


Fig. 2. (color online) (a) The tri-core PLs with separation of $L_s = 3T$. Linear splitting with fundamental modes at (b) $p = 0.5$, $h_D = -0.5$, (c) $p = 2$, $h_D = -0.5$, (d) $p = 2$, $h_D = -0.3$, and (e) $p = 2$, $h_D = -0.1$. In all the cases, the middle channel is excited. The numbers at the top right corner in panels (c)–(e) are the propagation length. (f) The coupling length depends on the defect strength under $p = 2$. Red circles [panels (c)–(e)] indicate the propagation dynamics (c)–(e), respectively. White circles mark the boundaries of the gap 1. All quantities are plotted in arbitrary dimensionless units.

we obtain the coupling length L_c versus h_D and plot the results in Fig. 2(f). As $h_D = -0.3$, L_c reaches its maximum 87.5. The coupling lengths are in agreement with a beam propagation simulation, the results are shown in Figs. 2(c) and 2(d). Note that the coupling coefficient can be controlled by the defect strength, and the curve presents the maximum values for a certain defect strength. It is very different from the one of the coupling coefficient versus the lattice modulation strength which is monotonous, referred to in Ref. [18]. All these findings are rather interesting, as they reveal that the splitting and combination dynamics can be finely tuned by the system's parameters.

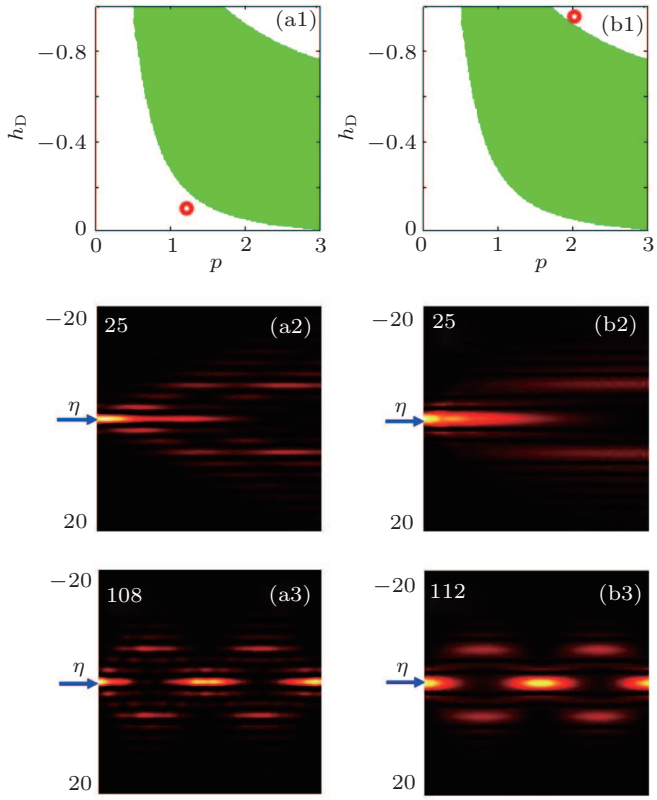


Fig. 3. (color online) (a1) the parameters of the tri-core PLs, marked by red circle $p = 1.2$, $h_D = -0.16$. (a2) linear diffraction (a3) nonlinear splitting happens when out of existence domain of linear splitting in defocusing media. (b1)–(b3) the parameters marked by red circle ($p = 2$, $h_D = -0.94$) in the focusing media, respectively. The input powers are $U_{in} = 0.01$ (a2), $U_{in} = 0.48$ (a3), $U_{in} = 0.01$ (b2), and $U_{in} = 0.55$ (b3). The numbers at the top left corner in panels (a2), (a3), (b2) and (b3) are the propagation length, and all quantities are plotted in arbitrary dimensionless units.

If we choose the parameters outside the linear splitting existence region, the beam will rapidly diffract. A natural question is whether we can make the splitting happen again according to nonlinearity while it disappears under the linear conditions. We choose the two groups of parameters shown in Figs. 3(a1) and 3(b1). At the circle $[(p, h_D) = (1.2, -0.16)]$ in Fig. 3(a1), the beam experiences diffraction [Fig. 3(a2)] at low power ($U_{in} = 0.01$). The defect modes touch the bottom of the first Bloch band, thus we assume a defocusing nonlinearity to lower the defect strength and pull the defect mode back to the photonic bandgap. With growing input power, less energy is transmitted to the hole space, and nonlinear splitting is reached at $U_{in} = 0.48$ [Fig. 3(a3)]. A similar situation is demonstrated at the circle $[(p, h_D) = (2, -0.94)]$ in Fig. 3(b1). However, we take advantage of a focusing nonlinearity to balance the diffraction because the defect strength causes the defect mode to touch the second Bloch band in this case. At $U_D = 0.55$, nonlinear splitting is obtained [Fig. 3(b3)] while it quickly spreads out [Fig. 3(b2)] to the linear region. Thus, the domain for splitting is enlarged when nonlinearity is introduced; therefore, it will help to better understand nonlinear coherent beam beating.

4. Multi-color linear splitting dynamics

Finally, multi-color linear splitting and active signal control are proposed in the tri-core PLs. Recall that the discussion so far assumes a single wavelength. In photonic lattices, defect modes with different wavelengths can be supported in defect sites, which differs from the case of photonic crystals.[4] A set of equations describes the multi-color beam linear evolution at different vaccum wavelengths λ_m:

$$\mathrm{i}\frac{\partial q_m}{\partial \xi} = -\frac{\xi_s \lambda_m}{4\pi n_0 \eta_s^2}\frac{\partial^2 q_m}{\partial \eta^2} - \frac{2\pi \xi_s p_s}{\lambda_m} pR(\eta)\, q_m, \qquad (3)$$

where $\eta_s = 1$ μm and $\xi_s = 1$ mm are characteristic values, respectively; n_0 is the average refractive index of the medium and $p_s = 1\,\mathrm{e}^{-4}$ is the normalized value of refractive index vibration.

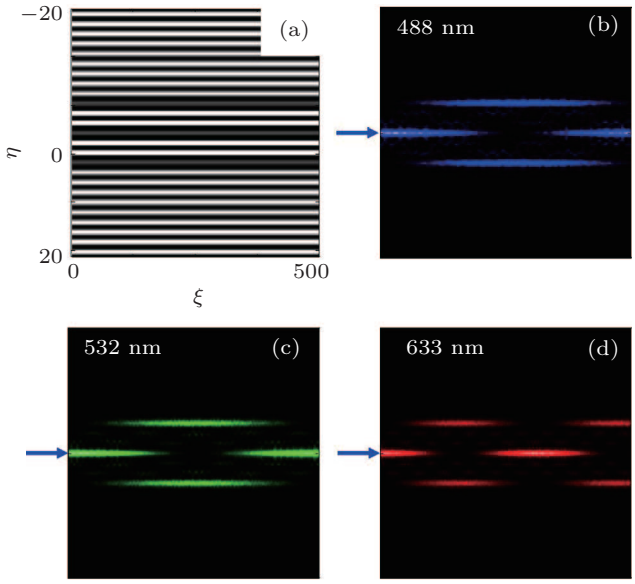


Fig. 4. (color online) Splitting dynamics of a light beam with different wavelengths in the same setting of the tri-core PLs ($h_D = -0.6$, $p = 2$, $z = 500$) shown in panel (a). Panels (b)–(d) show the beam propagations with the wavelengths 488 nm, 532 nm, and 633 nm, respectively.

Figure 4 shows the splitting dynamics of a probe beam at 488 nm, 532 nm and 633 nm in the same photonic structure. Since the beam has three different wavelengths, the splitting

dynamics differ due to different coupling lengths. The coupling length L_c becomes small as the wavelength increases, as shown in Figs. 4(b)–4(d). The beam energy for different wavelengths hits different location sites. For example, under finely designed device length ($L = 500$), the 488-nm probe beam distributes its energy in the central defect site while the 633 nm is located at the neighbor defect sites after the same propagation length. This feature has a potential for applications in signal splitting of white-light or fs-second laser light.

5. Conclusion

We demonstrated the main features of light splitting and combining between three low-index defect sites in photonic lattices. The parameter domain for the existence of splitting is determined. The coupling lengths can be adjusted by the lattice modulation strength, the defect strength and the defect site spacing. Under the same conditions, nonlinear splitting is demonstrated while it disappears in the linear case. Finally, we showed that multi-color splitting can be achieved in the micron scale in defective photonic lattices. These results might be useful for all-optical manipulation and photonic structure engineering.

References

[1] Christodoulides D N, Lederer F and Silberberg Y 2003 *Nature* **424** 817
[2] Tang X G, Liao J K, Li H P, Zhang L, Lu R G and Liu Y Z 2011 *Chin. Opt. Lett.* **9** 012301
[3] Zhou J T, Shen H J, Jia R, Liu H M, Tang Y D, Yang C Y, Xue C L and Liu X Y 2011 *Chin. Opt. Lett.* **9** 082303
[4] Makasyuk I, Chen Z G and Yang J K 2006 *Phys. Rev. Lett.* **96** 223903
[5] Fedele F, Yang J K and Chen Z G 2005 *Opt. Lett.* **30** 1506
[6] Wang X S, Chen Z G and Yang J K 2006 *Opt. Lett.* **31** 1887
[7] Wang X S and Chen Z G 2009 *Opt. Express* **17** 16927
[8] Mekis A, Chen J C, Kurland I, Fan S H, Villeneuve P R and Joannopoulos J D 1996 *Phys. Rev. Lett.* **77** 3787
[9] Yang X Y, Zheng J B and Dong L W 2011 *Chin. Phys. B* **20** 034208
[10] Zhou K Y, Guo Z Y, Muhammad A A and Liu S T 2010 *Chin. Phys. B* **19** 014201
[11] Christodoulides D N and Eugenieva E D 2001 *Phys. Rev. Lett.* **87** 233901
[12] Smirnov E, Rüter C E, Stepic M, Shandarov V and Kip D 2006 *Opt. Express* **14** 11248
[13] Knight J C 2003 *Nature* **424** 847
[14] Friberg S R, Weiner A M, Silberberg Y, Sfez B G and Smith P S 1988 *Opt. Lett.* **13** 904
[15] Yariv A, Xu Y, Lee R K and Scherer A 1999 *Opt. Lett.* **24** 711
[16] Salgueiro J R and Kivshar Y S 2005 *Opt. Lett.* **30** 1858
[17] Fogli F, Saccomandi L, Bassi P, Bellanca G and Trillo S 2002 *Opt. Express* **10** 54
[18] Ye F, Kartashov Y V, Vysloukh V A and Torner L 2008 *Phys. Rev. A* **78** 013847
[19] Mori D and Baba T 2004 *Appl. Phys. Lett.* **85** 1101
[20] Chen L, Wang G P, Gan Q Q and Bartoli F J 2010 *Appl. Phys. Lett.* **97** 153115
[21] Chen L, Wang G P, Li X, Li W, Shen Y, Lai J and Chen S 2011 *Appl. Phys. B* **104** 653